

LOW-CARBON VEGETATION CONFIGURATION STRATEGIES FOR URBAN PARKS USING DEEP LEARNING TECHNOLOGY

AN, Y.

*Academy of Fine Arts, ABa Teachers College, ABa, 623002 Sichuan, China
(e-mail: fjlgnaai4353@outlook.com)*

(Received 13th Aug 2025; accepted 10th Nov 2025)

Abstract. This study utilizes the DeepLabV3+ panoramic segmentation model based on ResNet50 to identify and quantitatively analyze the landscape elements in urban parks in China. The aim is to propose low-carbon vegetation configuration strategies to optimize park landscape design. By obtaining pictures of park landscape scenes and pre-training the model with the public ADE20K dataset, high-precision segmentation of landscape elements is achieved. The study quantitatively characterizes the landscape elements and focuses on analyzing the correlation between the Green Visibility Rate (GVI) and the vegetation proportion, as well as their impact on visitor satisfaction.

Keywords: *urban park, DeepLabV3+, GVI, landscape design, low-carbon vegetation*

Introduction

Urban parks are important parts of the urban green space system and essential places for citizens to relax and enjoy leisure activities, and also key components for improving the urban ecological environment and enhancing the quality of residents' lives. Urban park landscapes usually combine natural elements (such as vegetation, water bodies, and topography) with artificial structures (such as buildings, sculptures, and walkways), creating a harmonious unity of nature and humanity (Chiesura, 2004; Goličnik and Thompson, 2010). Traditional park landscape design mostly relies on subjective experience and qualitative analysis, making it difficult to meet the diverse needs of modern cities for landscape functionality and ecological benefits.

However, the improvement of deep learning technology has provided ways for the automatic identification and quantitative analysis of landscape elements. Notably, remarkable achievements have been made in tasks such as object detection (Zhao et al., 2017), image classification (Usamentiaga et al., 2022), and video understanding (Abbas et al., 2018). Through neural networks, deep learning automatically extracts and learns features from high-dimensional raw data (such as images), enabling efficient processing of complex visual information and offering powerful technical support for the identification and analysis of scene elements (Abbas et al., 2018). In urban park landscape design, the spatial characteristics of landscape elements (such as vegetation distribution, water body morphology, and building layout) are key factors affecting landscape quality and functionality (He et al., 2022). Traditional methods rely on manual surveys and subjective judgments, making it difficult to achieve large-scale and high-precision extraction of landscape elements. The introduction of deep learning technology provides new possibilities for the digitalization and refinement of landscape design.

In the field of scene element extraction and identification, various deep learning models have been widely applied and achieved remarkable results. For example, Faster R-CNN (Li et al., 2023) performs excellently in object detection tasks and can accurately locate various elements in the scene (such as buildings, vegetation, and roads). ResNet (Sarwinda et al., 2021) solves the gradient vanishing problem in the training of deep

networks through residual learning and is widely used in image classification and feature extraction tasks. The DeepLab series (Chen et al., 2024) (such as DeepLabV3+) combines dilated convolutions and encoder-decoder structures, which can accurately capture multi-scale context information and perform well in semantic segmentation tasks, suitable for element segmentation in complex scenes. U-Net (Li and Koo, 2024) stands out in medical image segmentation with its unique U-shaped structure and is also applied to the refined segmentation of landscape elements. Mask R-CNN (Quintus et al., 2023) adds an instance segmentation function on the basis of object detection, enabling both object localization and pixel-level segmentation, suitable for multi-element identification in complex scenes. These models have demonstrated strong capabilities in element extraction in highway scenes, urban landscapes, and natural environments, providing important tools for the digitalization and refinement of landscape design.

Based on advanced deep-learning models and combined with the characteristics of urban park landscapes, this study proposes an efficient and accurate method for landscape element extraction and quantitative analysis. Through deep-learning technology, large-scale and high-precision extraction of park landscape elements can be achieved, providing technical support for the digitalization and refinement of landscape design, as well as scientific basis for the ecological optimization and functional improvement of urban parks. The application of deep-learning technology not only promotes innovation in landscape design methods but also provides new research directions and practical paths for the sustainable development of urban green spaces. The objective of this study is to develop a deep learning-based method for accurate identification and quantitative analysis of urban park landscape elements, and to propose low-carbon vegetation configuration strategies to enhance landscape quality and visitor satisfaction.

Materials and methods

Visual elements of urban park landscape

The visual elements of urban park landscape are the basic units that make up the urban park landscape space, covering the scene-forming units such as the natural environment and artificial structures within the tourists' field of vision, including various elements such as the sky, vegetation, water bodies, terrain, buildings, and landscape ornaments. According to the different constituent elements of the objects, the urban park landscape elements can be divided into two major categories: natural landscape elements and cultural landscape elements (Zhou et al., 2022). Natural landscape elements include the sky, vegetation (trees, shrubs, ground cover), terrain, and water bodies. Cultural landscape elements include buildings, landscape ornaments (e.g., sculptures, seats, street lamps), roads and pavements, and amusement facilities. This study mainly focuses on the natural landscape elements of urban park landscapes. The natural landscape elements include the sky, vegetation, terrain, and water bodies. Among them, the vegetation can be further divided into trees, shrubs, and ground-cover plants. Buildings mainly refer to nearby residential buildings, visitor centers, etc.; landscape ornaments include small-scale facilities such as sculptures, seats, and street lamps; roads and pavements involve walkways, bicycle paths, and square pavements; amusement facilities cover children's playgrounds and fitness equipment. Through this classification method, the visual elements of the urban park landscape space can be more clearly analyzed, providing a scientific basis for landscape design and planning.

Combined with the characteristics of the visual elements of the urban park landscape, this study conducts a quantitative analysis of the visual elements of the urban park landscape space from three aspects: element characteristics, structural characteristics, and attribute characteristics.

1) Element characteristics mainly represent the characteristics of the constituent elements of the urban park landscape scene, mainly considering the element composition and element proportion. The element composition of the park landscape mainly includes vegetation, water bodies, buildings, roads, and paths. The element proportion of the park landscape takes into account the vegetation coverage rate, the proportion of water-body area, the proportion of hard pavements, etc.

2) Structural characteristics mainly reflect the spatial structural characteristics of the elements in the urban park landscape space. The Green Visibility Rate (GVI), Blue Visibility Rate, and sky openness index are the main parameters that affect the spatial structural characteristics (Sun et al., 2023).

3) Attribute characteristics mainly consider indicators such as color elements, color richness, and dominant color spectrum (Kang and Liu, 2022). The green-dominated landscape of urban parks may give people a feeling of nature and tranquility. The Green Visibility Rate (GVI) is calculated as the proportion of visible green vegetation in the field of view. The Blue Visibility Rate refers to the proportion of visible sky, and the Sky Openness Index quantifies the degree of sky exposure. The GVI was calculated using the area occupied by trees, shrubs, and ground cover in the highway landscape scene pictures (Xu and Niu, 2024). The calculation formula is as follows.

$$GVI = \frac{Area_q + Area_d}{Area_v} \times 100\% \quad (\text{Eq.1})$$

Here, $Area_q$ is the area occupied by trees and shrubs in the landscape scene; $Area_d$ is the area occupied by the ground cover in the landscape scene; $Area_v$ is the field of view.

We use mIoU (mean Intersection over Union) and PQ (Panoptic Quality) to measure the model's performance in semantic segmentation and panoptic segmentation tasks (Khoshboresh-Masouleh and Shah-Hosseini, 2021).

$$mIoU = \frac{1}{k+1} \sum_{i=0}^k \frac{TP}{FN + FP + TP} \quad (\text{Eq.2})$$

$$PQ = \frac{\sum_{(p,g) \in TP} IoU(p,q)}{|TP| + \frac{1}{2}|FP| + \frac{1}{2}|FN|} \quad (\text{Eq.3})$$

In the *Eqs. (2) and (3)*, TP stands for true positive; FP stands for false positive, which means the prediction is incorrect; FN stands for false negative.

The Sky Openness Index (SOI), which quantifies the degree of sky exposure considering vertical angles, was also computed using the *Eq. (4)*:

$$SOI = (\sum \cos \theta_i) / N \quad (\text{Eq.4})$$

where θ_i is the vertical angle of sky pixel i , and N is the total number of sky pixels.

Panoramic segmentation model

DeepLabV3+ segmentation model

DeepLabV3+ is an advanced semantic segmentation model proposed by Google (Chen et al., 2024). The basic structure of the DeepLabV3+ model is shown in *Figure 1*. As shown in *Figure 1*, the model features an encoder-decoder architecture specifically designed for capturing multi-scale contextual information while maintaining fine-grained spatial details.

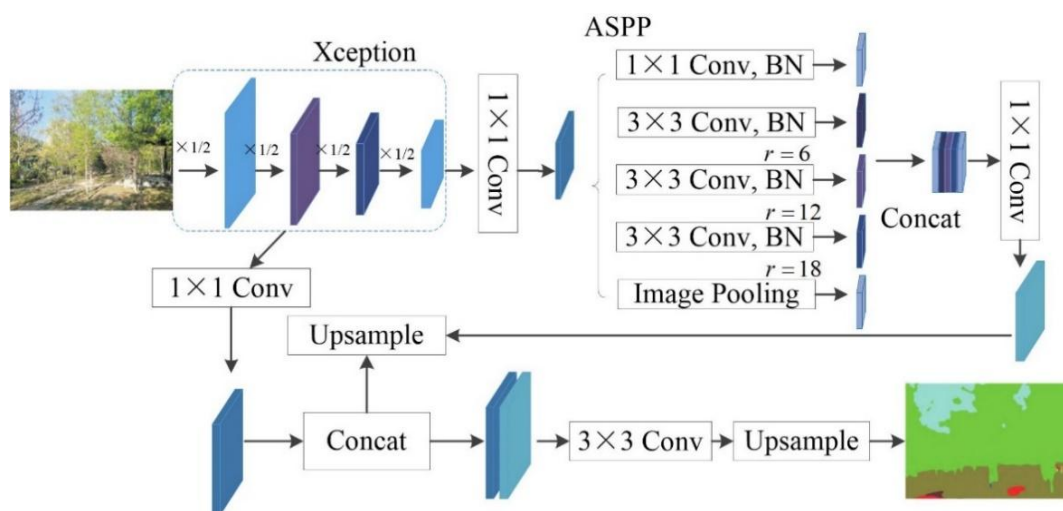


Figure 1. Basic principle of DeepLabV3+ segmentation model

The core structure of DeepLabV3+ consists of two parts: an encoder and a decoder. In the encoder part, a deep convolutional neural network (such as ResNet or Xception) is usually adopted as the backbone network to extract image features. The ResNet50 backbone used in this study consists of 50 layers organized into four sequential blocks, with each block containing multiple bottleneck residual layers that progressively extract features at different scales while preserving gradient flow through skip connections.

To expand the receptive field without increasing the number of parameters, the encoder introduces atrous convolution (Lu et al., 2024), which captures multi-scale information by setting different sampling rates. Atrous convolution expands the receptive field and maintains the feature map resolution by inserting "holes", which is suitable for capturing multi-scale context information; while non-atrous convolution gradually reduces the resolution through a traditional sliding window, which is suitable for efficiently extracting abstract features. *Figure 2* shows the difference between non-atrous convolution (standard convolution) and atrous convolution (dilated convolution) in the neural network.

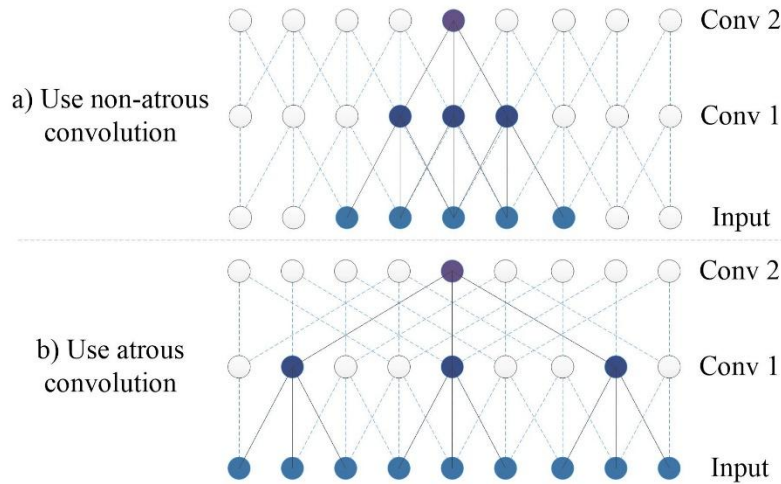


Figure 2. Network mechanism of void convolution and non-void convolution

Mathematically, atrous convolution expands the receptive field by inserting “holes” into the convolution kernel.

$$y[i] = \sum_k x[i + r \cdot k] \cdot w[k] \quad (\text{Eq.5})$$

Here, x and y represents the input and output feature map; w represents the weights of the convolution kernel; r represents the dilation rate; i and k represent the indices of the output and the convolution kernel respectively.

In addition, the encoder also adopts the Atrous Spatial Pyramid Pooling (ASPP) module (Qiu et al., 2022). It extracts multi-scale features by using multiple atrous convolutions with different sampling rates in parallel, thereby enhancing the model's adaptability to multi-scale objects.

$$y = \text{Concat}(y_1, y_2, y_3, y_4) \quad (\text{Eq.6})$$

Here, y_{1-4} are the outputs of the atrous convolutions of each convolutional layer in the ASPP.

In the decoder part, by fusing the low-level features and high-level semantic features extracted by the encoder, the image resolution is gradually restored to generate high-precision segmentation results. The model is trained using the cross-entropy loss function.

$$y_{\text{decoder}} = \text{Conv}(\text{Concat}(\text{Upsample}(y_{\text{high}}), y_{\text{low}})) \quad (\text{Eq.7})$$

Here, y_{high} represents the high-level semantic features, which are the outputs of the ASPP; y_{low} represents the low-level features, which are the shallow outputs of the backbone network.

DeepLabV3+ is trained using the Cross-Entropy Loss function, and the Eq. (8) is as follows:

$$L = -\sum_{i=1}^N \sum_{c=1}^C y_{i,c} \cdot \log(p_{i,c}) \quad (\text{Eq.8})$$

where N is the total number of pixels; C is the total number of classes; $y_{i,c}$ is the ground-truth label (one-hot encoded) of pixel i ; $p_{i,c}$ is the probability that the model predicts pixel i belongs to class c .

This architecture enables DeepLabV3+ to effectively combine deep semantic information with shallow spatial details, making it particularly suitable for segmenting complex urban park landscapes where both contextual understanding and boundary precision are crucial for accurate element identification.

ResNet50 Convolutional Neural Network

ResNet is a deep-learning model that introduces the idea of residual learning into traditional Convolutional Neural Networks (CNNs) (Sarwinda et al., 2021). The residual block implements the idea of residual learning through a two-branch design of identity mapping and residual mapping. See *Figure 3* for details. The identity mapping retains the original information of the input features, while the residual mapping learns the difference between the input and the output. The output of the residual block is calculated by:

$$y = F(x, \{W_i\}) + x \quad (\text{Eq.9})$$

where, x is the input feature; $F(x, \{W_i\})$ is the output of the residual mapping; y is the final output of the residual block; and x is the output of the identity mapping.

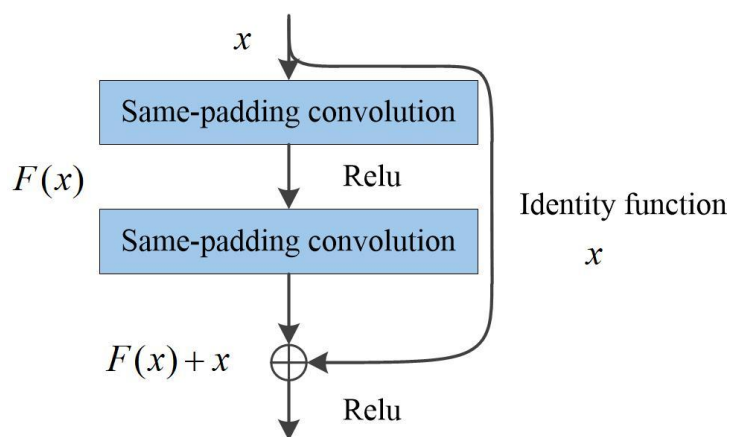


Figure 3. Double branch design of residual block

The loss function of the ResNet network is $F(X, W)$, and the gradient value of its backpropagation is shown below.

$$Loss = F(X, W) \quad (\text{Eq.10})$$

$$\frac{\partial Loss}{\partial X} = \frac{\partial F(X, W)}{\partial X} \quad (\text{Eq.11})$$

The loss function and gradient of the layer neural network of the i -th layer are shown below:

$$Loss = F_n(X_n, W_n), L_n = F_{n-1}(X_{n-1}, W_{n-1}), \dots, L_2 \quad (\text{Eq.12})$$

$$\frac{\partial X_{i+1}}{\partial X_i} = \frac{\partial X_i + \partial F(X_i, W_i)}{\partial X_i} = 1 + \frac{\partial F(X_i, W_i)}{\partial X_i} \quad (\text{Eq.13})$$

The network structure of ResNet50 is shown in *Figure 4*. Its network structure is designed based on the residual block and has a depth of 50 layers. The network structure of ResNet-50 consists of 4 convolutional blocks, and each convolutional block contains multiple bottleneck residual blocks. The 1×1 , 3×3 , and 1×1 convolutional layers are used to extract features, and the skip connection is utilized to alleviate the problem of gradient vanishing. Finally, the classification results are output through global average pooling and a fully-connected layer.

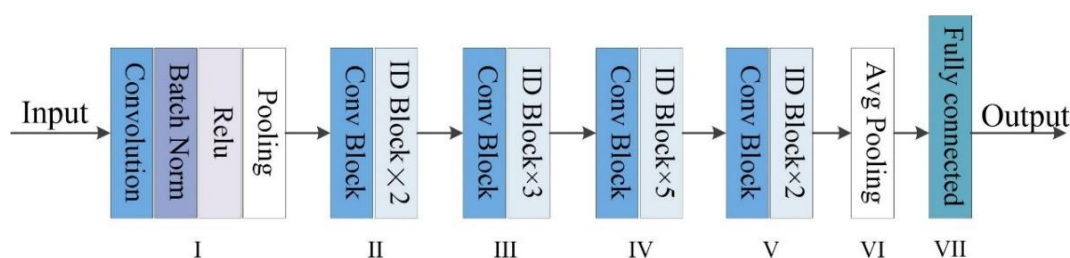


Figure 4. Structure of ResNet50 convolutional neural network

Results

Data set and evaluation index

This study takes the Binhe Park in northern China as the research object. Located in the city's central area, this park is one of the important waterfront landscapes in the urban area. A map of the park is provided in *Figure 5*. The total area of the park is 58.3 hectares, with the water surface area accounting for 15.7 hectares. The landscape design in the park integrates natural and cultural elements, featuring typical characteristics of an urban park. The established landscape nodes in the park usually serve to guide the gathering of tourists. The sample plots selected in this study include four types of spaces: trails, green areas, buildings, and lakes, ensuring the typicality and diversity of the sample plots. The main tree species in the park include *Populus tomentosa*, *Ginkgo biloba*, *Platycladus orientalis*, *Pinus tabuliformis*, etc. The selected sample plots need to contain both natural (such as soil, vegetation, and water bodies) and artificial (such as buildings, paths, and facilities) landscape elements.

This study uses Baidu's panoramic static image API combined with web-crawling technology and UAV-captured images to obtain a large number of landscape scene images of the park, aiming to achieve a quantitative representation of landscape elements. The field of view was calculated based on known camera parameters and shooting angles. After removing images with repeated shooting, large differences in light perception, and many irrelevant factors, 200 panoramic images that can restore the full view of the park

were selected as samples for this study. In this experiment, the publicly available ADE20K dataset was used to pre-train the DeepLabV3+ segmentation model to ensure the model's segmentation performance in complex scenarios.



Figure 5. Geographical location of the park

All images were acquired using standardized protocols: Baidu panoramic images were captured with a focal length of 35 mm (equivalent) on a full-frame sensor, while UAV images used a 24 mm lens with known altitude parameters (30-50 meters). For Baidu panoramic images, the horizontal FOV (the field of view) was 80°, while UAV images maintained a 60° FOV.

Landscape element identification

The trained model was used for validation, and the calculated mIoU and PQ values are shown in *Figure 6*. The model achieved quantitatively good segmentation results in the urban park scenario, with both mIoU and PQ reaching high levels. This indicates that the model can accurately identify and segment various landscape elements in the park, such as the sky, vegetation, buildings, and water bodies.

As the number of training iterations increased, although both mIoU and PQ fluctuated, their overall trend was upward. They reached the optimal values at around 190,000 iterations, where the PQ was 0.564 and the mIoU was 77.8.

Additionally, a confusion matrix was generated to analyze classification errors between different landscape element categories. To further evaluate model accuracy, we conducted a confusion matrix analysis. High IoU values for sky (89.2%) and buildings (83.7%), indicating strong segmentation of distinct elements. Moderate performance for trees, with lower values for shrubs and grasses, reflecting the challenge of fine-grained vegetation classification. Primary misclassification occurred between shrubs and grasses (15.3% confusion), and between soil and paved surfaces (12.7%). While some confusion remains between shrubs and grasses due to their visual similarity in two-dimensional imagery, the fine-tuning process has substantially enhanced inter-class discrimination compared to the baseline model.

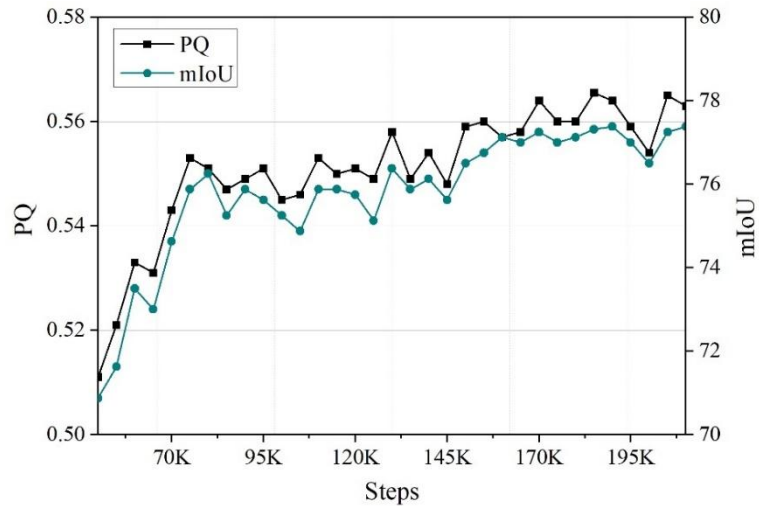


Figure 6. Panoptic segmentation results of the urban park scene

During training, observed fluctuations in mIoU and PQ are characteristic of the stochastic optimization process and do not indicate model failure. As training progressed, both metrics stabilized and converged to high values after approximately 190,000 iterations, confirming the model's ability to consistently identify landscape elements.

The trained panoptic segmentation model was used to identify urban park landscape elements. By considering the positional relationships and forms of natural landscape elements such as the sky, shrubs, and ground cover, as well as artificial landscape elements like fences and buildings in the park scene, the recognition results are shown in *Figure 7*.

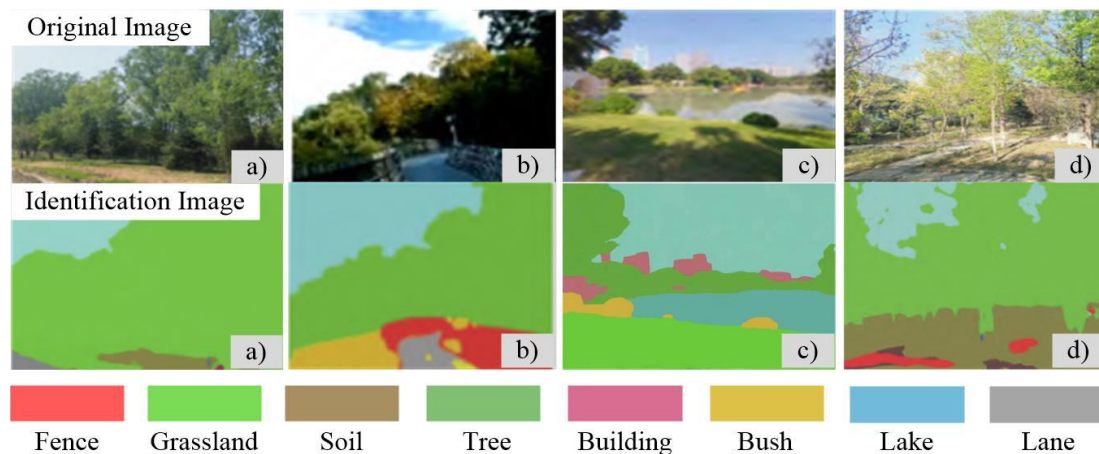


Figure 7. Recognition results of the panoptic segmentation model

Figure 7 presents the recognition results of the panoptic segmentation model for urban park landscape elements. Through the segmentation output of the model, the distribution of various landscape elements in the park scene can be clearly observed, including the sky, vegetation (such as trees, shrubs, and grasslands), buildings, water bodies, fences, etc.

As the most common natural element in park landscapes, the sky dominates in most scenes. Its recognition accuracy is high, with clear boundaries and obvious spatial features. Green vegetation is the focus of park landscape design, mainly consisting of trees, shrubs, and grasslands. The model can identify the overall distribution of vegetation well. However, in some scenes, nearby trees and shrubs are misclassified as grasslands, indicating certain errors. This may be due to the strong hierarchical nature of nearby vegetation, causing difficulties for the model in detailed segmentation. Buildings, as artificial landscape elements, have obvious shape features and are relatively easy to recognize. The model can accurately segment the outlines of buildings. Water bodies (such as lakes and rivers) play an important role in park landscapes. The model can identify the boundaries of water bodies well, and the segmentation results are relatively accurate. However, elements such as fences and soil frequently show blurred boundaries and misclassification in the recognition results. This may be because the shapes and textures of these elements are relatively complex, making it difficult for the model to accurately distinguish them during segmentation.

Overall, the recognition accuracy of the model for urban park landscape scene images reaches 78.5%, and the recognition time for each image during the processing is about 1 second. This greatly improves the recognition and processing speed of park landscape scenes, provides data support for the quantitative characterization of visual elements in urban park landscape spaces in the next step, and offers a scientific basis for landscape design and planning. The model demonstrates improved ability to distinguish between trees, shrubs, and grasses after fine-tuning on a more detailed dataset.

Regarding computational efficiency, the proposed model processes each image in approximately 1 second on an NVIDIA RTX 3080 GPU. This represents a significant improvement over comparative models: DeepLabV3 (1.8 seconds), U-Net (2.3 seconds), and Mask R-CNN (3.1 seconds) under identical hardware and image resolution conditions. The 56-68% reduction in processing time demonstrates the practical advantage of our approach for large-scale park landscape analysis applications.

Quantification and evaluation of landscape elements

In this study, 200 park landscape scene pictures (numbered from Picture 1 to Picture 200) in the experimental area were selected for the analysis of element features and spatial features. In addition to the Green Visibility Rate (GVI), the Blue Visibility Rate (BVR) and Sky Openness Index (SOI) were also calculated and analyzed to comprehensively evaluate the visual and spatial characteristics of the park landscape. The rationality of the urban park scene layout structure design was analyzed based on the composition and proportion of urban park landscape elements.

Quantitative characterization of spatial visual elements was carried out on the representative pictures of the urban park environment. The landscape elements involved included various elements such as the sky, lake water, buildings, shrubs, grasslands, trees, soil, fences, etc. According to the element types, they can be divided into natural landscapes, buildings, landscape sculptures and facilities, and roads and pavements. The proportion and distribution of these categories in the scene pictures are specifically shown in *Figure 8*.

Furthermore, the Blue Visibility Rate (BVR), defined as the proportion of visible sky area in the field of view, was calculated for each scene. The analysis revealed that scenes with higher BVR (>30%) and SOI (>0.6) were predominantly located in open areas such as lawns and squares, where visitors reported higher satisfaction scores (average 4.2/5).

In contrast, areas with dense tree canopies showed lower BVR (<15%) and SOI (<0.3), which provided better shading but sometimes led to perceptions of "gloominess" when vegetation hierarchy was poor. These findings demonstrate that BVR and SOI serve as effective indicators for evaluating spatial openness and visual comfort in urban park design.

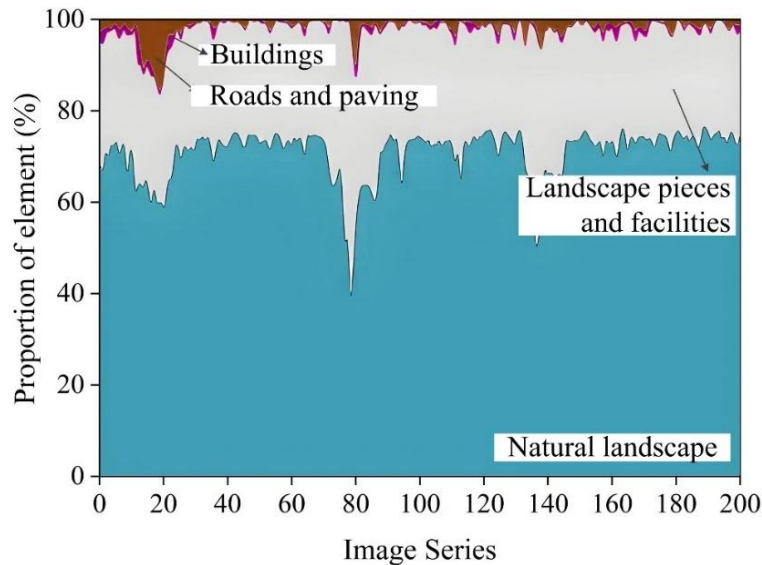


Figure 8. Distribution of landscape elements in the park scene picture

Through quantitative analysis, it is possible to intuitively observe the proportion and spatial distribution characteristics of various landscape elements in the park scene. Natural landscape elements (such as the sky, lake water, and vegetation) account for a relatively large proportion in the park scene. In particular, the sky and vegetation are widely and evenly distributed, which indicates that the park design emphasizes the integration of natural elements and creates a good ecological environment. As artificial landscape elements, buildings are relatively concentrated in distribution and are usually located at the edges of the park or in specific functional areas (such as the visitor center and rest areas). Their proportion is relatively low, but they play an important functional support role in the spatial layout. Landscape sculptures (such as sculptures and street-lights) and facilities (such as fences and seats) account for a small proportion in the scene, but are relatively evenly distributed, adding a humanistic atmosphere and functionality to the park. Roads and pavement elements occupy a certain proportion in the park scene and are mainly distributed in areas such as walkways and squares. The rationality of their design is closely related to the tourists' visiting experience. Overall, the results in *Figure 8* reflect the reasonable allocation and spatial distribution of various elements in the park landscape design, guiding the optimization of the landscape element structure and the configuration of greening plants in park landscape design.

In this study, the green vegetation in the highway landscape space was identified through panoptic segmentation.

When using the panoptic segmentation model to process park landscape pictures, the proportions of ground cover, trees and shrubs are calculated to obtain the analysis results of the GVI. *Figure 9* shows the correlation between the GVI and the proportion of vegetation. By conducting a correlation analysis between the GVI and the proportions of

different types of vegetation in the highway scene, it can be seen that the proportion of trees and shrubs has a relatively strong correlation with the overall trend of the GVI, with a correlation coefficient of 0.87. In contrast, the proportion of ground cover has a relatively poor correlation with the overall trend of the GVI ($R^2=0.29$). This also indicates that the impact of the ground-cover proportion on the GVI is mainly concentrated in scenes with a low GVI. Obviously, the change trend of the GVI is more closely related to the proportion of trees and shrubs.

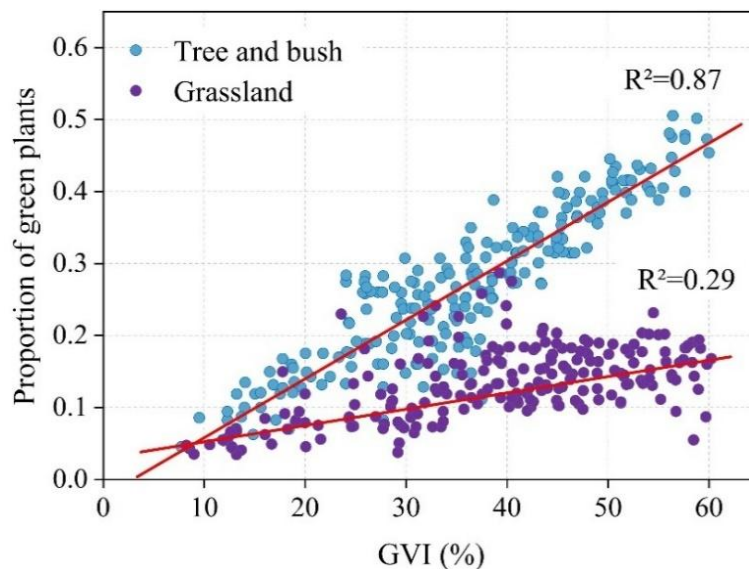


Figure 9. Correlation between green visual rate and vegetation proportion

In conclusion, in the landscape design of urban parks, measures such as plant transplantation and replanting can be taken. Based on the analysis of the GVI in each area of the park, the greening configuration and spatial layout can be adjusted to enhance the sense of hierarchy and visual richness of the park landscape, providing tourists with a good visual experience and aesthetic feeling. At the same time, increasing the GVI is mainly achieved by increasing the proportion of trees and shrubs, which provides theoretical basis and practical guidance for the landscape design of urban parks. The rationality of the urban park scene layout structure design was analyzed based on the composition and proportion of urban park landscape elements. Through the reasonable configuration of trees and shrubs, the greening effect and ecological value of the park can be effectively improved, creating a more pleasant recreational environment.

Discussion

To comprehensively evaluate the satisfaction of urban park landscapes, this study conducted a landscape satisfaction evaluation of tourists in the park through a questionnaire survey (conducted in June 2024, with 150 participants, using an online and on-site combined method). The questionnaire used a Likert 5-point scale, where 1 represents "very dissatisfied" and 5 represents "very satisfied". The evaluation indicators involved in the questionnaire cover four aspects: landscape aesthetics, functional facilities, ecological environment, and social culture.

The findings of this study align with international research on the relationship between Green View Index (GVI) and visitor satisfaction. For instance, Sun et al. (2023), in their study of coastal streets in Qingdao, also found a positive correlation between GVI and visual comfort, which is consistent with our conclusion that visitor satisfaction significantly improves when GVI exceeds 40%. However, compared to the landscape quality evaluation framework proposed by Kang and Liu (2022), our results emphasize a more pronounced impact of vegetation hierarchy on satisfaction, particularly in scenes with high GVI but low satisfaction scores. This underscores the necessity of integrating visual hierarchy and aesthetic design into vegetation configuration, beyond merely increasing green quantity. Furthermore, our segmentation approach using DeepLabV3+ demonstrates higher computational efficiency compared to traditional methods like U-Net and Mask R-CNN used in similar landscape studies (Quintus et al., 2023; Li and Koo, 2024), providing a more practical solution for large-scale park landscape analysis.

The GVI is an important indicator for measuring the visibility of green vegetation in the landscape and is closely related to tourists' satisfaction. To explore the impact of plant configuration on tourists' satisfaction, *Table 1* shows the statistical results of the average GVI of scene pictures under different satisfaction levels. As the GVI increases, tourists' satisfaction shows an upward trend. Specifically, the average GVI of scenes with a "very dissatisfied" satisfaction level is 16.8%, while the average GVI of scenes with a "very satisfied" satisfaction level reaches or exceeds 50%. This indicates that a higher GVI can significantly improve tourists' satisfaction with the park landscape. However, the table also shows that in some scenes, although the GVI is high, tourists' satisfaction is still low, which may be related to the hierarchy and aesthetics of the vegetation and the overall coordination of the landscape design.

Table 1. Street green visibility rate satisfaction levels

Degree of Satisfaction	Average GVI
1	16.8%
2	23.4%
3	36.0%
4	45.1%
5	50.3%

Figure 10 presents the results of a correlation analysis between the GVI and the proportion of vegetation. As can be seen from the figure, with the increase in the GVI, tourists' satisfaction shows a fluctuating upward trend. Especially in scenes where the GVI exceeds 40%, tourists' satisfaction significantly improves. However, in some individual scenes, despite a high GVI, tourists' satisfaction remains low. This may be due to poor vegetation hierarchy or lack of aesthetics (such as overgrown weeds and uneven distribution of trees and shrubs).

Overall, the results in *Figure 10* indicate that increasing the proportion of trees and shrubs is an effective way to enhance the GVI and tourists' satisfaction. However, in the vegetation configuration, attention should also be paid to hierarchy and aesthetics to ensure the overall coordination and attractiveness of the landscape design.

Combined with the visualization results of the GVI in *Figure 11* and the on-site investigation results, corresponding green plant configuration strategies for urban parks can be proposed to optimize the landscape design and enhance tourists' satisfaction.

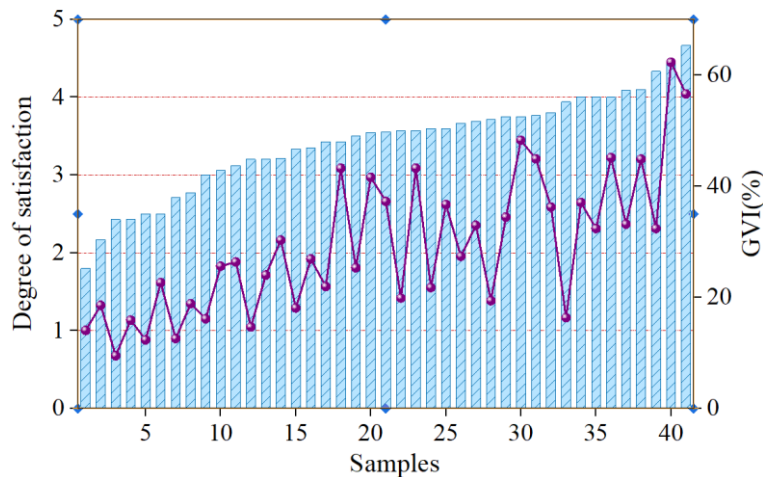


Figure 10. The relationship between GVI and satisfaction in some scene pictures

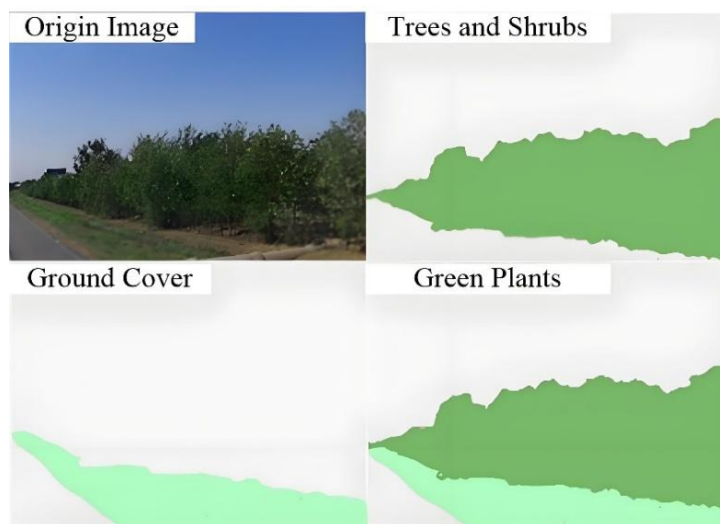


Figure 11. Example of green visual rate visualization results

First, the proportion of trees and shrubs should be increased to enhance the GVI. The results show that there is a strong correlation between the GVI and the proportion of trees and shrubs. This indicates that increasing the proportion of trees and shrubs is the key to enhancing the GVI. Therefore, in park design, the planting density of trees and shrubs should be increased first, especially in the main activity areas for tourists (such as around walkways and squares) to enhance the visual hierarchy and sense of space enclosure.

Second, the hierarchy and aesthetics of the vegetation need to be optimized. The visualization results of the GVI show that although the GVI in some scenes is high, tourists' satisfaction is still low. This may be due to the poor hierarchy or lack of aesthetics of the vegetation. Therefore, in the green plant configuration, attention should be paid to the hierarchical design of the vegetation. For example, in the tree layer, tree species with beautiful shapes and large crowns (such as ginkgo and Chinese scholar-tree) should be selected as the upper-layer vegetation; in the shrub layer, shrubs with strong ornamental value (such as forsythia and crape myrtle) should be planted to enrich the landscape color;

in the ground-cover layer, low-maintenance and trampling-resistant ground-cover plants (such as lawns and dwarf lilyturf) should be selected to ensure that the ground cover is neat and beautiful.

Finally, the vegetation should be reasonably arranged in combination with functional areas. According to the landscape element distribution analysis, the layout of the vegetation should be combined with the functional areas of the park. For example, trees with good shading effects should be planted in the rest areas, and low-growing shrubs should be planted in the children's play areas to provide a safety barrier, so as to improve the functionality of the park and the tourists' experience. Through the above strategies, the GVI and landscape quality of urban parks can be effectively improved, creating a more pleasant recreation environment for tourists.

Conclusion

This study uses the DeepLabV3+ panoramic segmentation model to identify and quantitatively analyze the landscape elements of urban parks, reaching the following conclusions. First, increasing the proportion of arbors and shrubs is an effective way to enhance the GVI. There is a strong correlation between the proportion of arbors and shrubs and the GVI. Second, the hierarchy and aesthetics of vegetation have an important impact on tourists' satisfaction. Although the GVI in some scenes is high, poor vegetation hierarchy or lack of aesthetics can lead to a decline in tourists' satisfaction. Therefore, in park landscape design, attention should be paid to the configuration of arbors and shrubs, optimize the vegetation hierarchy, and select tree species and ground-cover plants with strong ornamental value to enhance the visual appeal and ecological value of the landscape. Finally, there is a positive correlation between the improvement of the GVI and tourists' satisfaction. Especially in scenes where the GVI exceeds 40%, tourists' satisfaction significantly improves. This study provides theoretical basis and practical guidance for the low-carbon vegetation configuration and landscape optimization of urban parks, which is helpful for creating a more pleasant urban green space. Future work will focus on integrating multi-source data and improving model interpretability for broader application.

Funding. Special fund for social Science undertakings of Aba Prefecture: Research on the feature identification and protective construction strategy of red landscape in Aba Section of Long March National Cultural Park (ABKT2023053). Aba Intangible Cultural Heritage Innovation and Development Research Center – the Key Research Base of Humanities and Social Sciences (AS-XJPT2024-2).

REFERENCES

- [1] Abbas, Q., Ibrahim, M. E., Jaffar, M. A. (2018): Video scene analysis: an overview and challenges on deep learning algorithms. – *Multimedia Tools and Applications* 77(16): 20415-20453. <https://doi.org/10.1007/s11042-017-5438-7>.
- [2] Chen, H., Qin, Y., Liu, X., Wang, H., Zhao, J. (2024): An improved DeepLabv3+ lightweight network for remote-sensing image semantic segmentation. – *Complex & Intelligent Systems* 10(2): 2839-2849. <https://doi.org/10.1007/s40747-023-01304-z>.
- [3] Chiesura, A. (2004): The role of urban parks for the sustainable city. – *Landscape and Urban Planning* 68(1): 129-138. <https://doi.org/10.1016/j.landurbplan.2003.08.003>.

- [4] Goličnik, B., Thompson, C. W. (2010): Emerging relationships between design and use of urban park spaces. – *Landscape and Urban Planning* 94(1): 38-53. <https://doi.org/10.1016/j.landurbplan.2009.07.016>.
- [5] He, M., Wang, Y., Wang, W. J., Xie, Z. (2022): Therapeutic plant landscape design of urban forest parks based on the Five Senses Theory: A case study of Stanley Park in Canada. – *International Journal of Geoheritage and Parks* 10(1): 97-112. <https://doi.org/10.1016/j.ijgeop.2022.02.004>
- [6] Kang, N., Liu, C. (2022): Towards landscape visual quality evaluation: methodologies, technologies, and recommendations. – *Ecological Indicators* 142: 109174. <https://doi.org/10.1016/j.ecolind.2022.109174>.
- [7] Kazimi, B., Thiemann, F., Sester, M. (2019): Semantic segmentation of manmade landscape structures in digital terrain models. – *ISPRS Annals of the Photogrammetry, Remote Sensing and Spatial Information Sciences* 4: 87-94. <https://doi.org/10.5194/isprs-annals-IV-2-W7-87-2019>.
- [8] Khoshboresh-Masouleh, M., Shah-Hosseini, R. (2021): Building panoptic change segmentation with the use of uncertainty estimation in squeeze-and-attention CNN and remote sensing observations. – *International Journal of Remote Sensing* 42(20): 7798-7820. <https://doi.org/10.1080/01431161.2021.1966853>.
- [9] Li, W., Li, Z., Wei, Y., Gong, C., Zhang, M., Chen, L. (2023): Square ancient sites detection in typical regions of the Mongolian plateau using improved faster R-CNN from Google Earth high-resolution images. – *International Journal of Remote Sensing* 44(17): 5207-5227. <https://doi.org/10.1080/01431161.2023.2244641>.
- [10] Li, J., Koo, B. (2024): Application of U-Net remote sensing data in ecological landscape restoration planning and pollution prevention. – *International Journal of Environment and Pollution* 75(1): 1-20. <https://doi.org/10.1504/IJEP.2024.143454>.
- [11] Lu, Y., Tao, X., Jiang, F., Du, J., Li, G., Liu, Y. (2024): Image recognition of rice leaf diseases using atrous convolutional neural network and improved transfer learning algorithm. – *Multimedia Tools and Applications* 83(5): 12799-12817. <https://doi.org/10.1007/s11042-023-16047-9>.
- [12] Puttagunta, M., Ravi, S. (2021): Medical image analysis based on deep learning approach. – *Multimedia Tools and Applications* 80(16): 24365-24398. <https://doi.org/10.1007/s11042-021-10707-4>.
- [13] Qiu, Y., Liu, Y., Chen, Y., Zhang, J., Zhu, J., Xu, J. (2022): A2SPPNet: Attentive atrous spatial pyramid pooling network for salient object detection. – *IEEE Transactions on Multimedia* 25: 1991-2006. <https://doi.org/10.1109/TMM.2022.3141933>.
- [14] Quintus, S., Davis, D. S., Cochrane, E. E. (2023): Evaluating Mask R-CNN models to extract terracing across oceanic high islands: A case study from Sāmoa. – *Archaeological Prospection* 30(4): 477-492. <https://doi.org/10.1002/arp.1909>.
- [15] Sarwinda, D., Paradisa, R. H., Bustamam, A., Anggia, P. (2021): Deep learning in image classification using residual network (ResNet) variants for detection of colorectal cancer. – *Procedia Computer Science* 179: 423-431. <https://doi.org/10.1016/j.procs.2021.01.025>.
- [16] Song, T., Lu, G. (2024): Urban landscape modeling and algorithms under machine learning and remote sensing data. – *Earth Science Informatics* 17(3): 2303-2316. <https://doi.org/10.1007/s12145-024-01293-8>.
- [17] Sun, D., Ji, X., Gao, W., Zhou, F., Yu, Y., Meng, Y., Yang, M., Lin, J., Lyu, M. (2023): The relation between green visual index and visual comfort in Qingdao coastal streets. – *Buildings* 13(2): 457. <https://doi.org/10.3390/buildings13020457>.
- [18] Usamentiaga, R., Lema, D. G., Pedrayes, O. D., Garcia, D. F. (2022): Automated surface defect detection in metals: a comparative review of object detection and semantic segmentation using deep learning. – *IEEE Transactions on Industry Applications* 58(3): 4203-4213. <https://doi.org/10.1109/TIA.2022.3151560>.

- [19] Xu, X., Niu, L. (2024): Analysis of Influencing Factors of Green View Index Based on Street View Segmentation. – *The International Archives of the Photogrammetry, Remote Sensing and Spatial Information Sciences* 48: 517-524.
<https://doi.org/10.5194/isprs-archives-XLVIII-4-2024-517-2024>.
- [20] Zhao, B., Feng, J., Wu, X., Yan, S. (2017): A survey on deep learning-based fine-grained object classification and semantic segmentation. – *International Journal of Automation and Computing* 14(2): 119-135. <https://doi.org/10.1007/s11633-017-1053-3>.
- [21] Zhou, L., Huang, X., Zhao, C., Pu, T., Zhang, L. (2022): Regional landscape transformation and sustainability of the rural homegarden agroforestry system in the Chengdu Plain, China. – *Regional Sustainability* 3(1): 68-81. <https://doi.org/10.1016/j.regsus.2022.04.001>.